PRE-CONCEPTUAL FUEL DESIGN CONCEPTS FOR THE CANADIAN SUPER CRITICAL WATER-COOLED REACTOR

M.H. McDonald[1,2], B. Hyland[2], H. Hamilton[2], L.K.H. Leung[2], N. Onder[2], J. Pencer[2] and R. Xu[2]
[1] McMaster University, Ontario, Canada
[2] Atomic Energy of Canada Limited, Chalk River Laboratories, Ontario, Canada

Abstract

The Canadian Supercritical Water Reactor (SCWR) reactor is in the pre-conceptual design phase, as is its fuel. This paper will discuss the currently envisaged Canadian SCWR fuel design and briefly describe its rationale. Physics, thermalhydraulics and fuel performance characteristics of the fuel are discussed and parameters such as coolant void reactivity, acceptable linear element ratings and fuel sheath temperatures are considered. Several different bundle concepts have been examined, including: bundles with the same sized fuel elements in each ring, bundles with smaller pins in the outer ring and bundles with internally-cooled annular fuel elements in the outer ring.

1. Introduction

Previous work has investigated the physics design of the PT-SCWR for uranium and thorium fuel options [1], [2]. The PT-SCWR reactor concept is discussed in previous papers, and elsewhere in these conference proceedings [1], [2], and therefore is not repeated here to conserve space. As the pre-conceptual design work continues, the physics and fuel design work is being expanded to look at more phenomena. Most of the previous physics work was relatively simple, and has been focussed mainly on fuel composition, exit burnup, and coolant void reactivity. As a starting point of the fuel design process presented here, the linear element ratings were calculated. These ratings were found to be too high in the initial 54-element bundle design. Two new bundle designs have been developed in order to reduce the linear element ratings, and are examined here. In the first design, the fuel in the outer ring is subdivided, creating more, smaller diameter fuel pins. The second design used internally-cooled annular fuel pellets, in which coolant flows through an axial hole in the centre of the pellets. The original 54-element bundle design and both new designs use homogeneous plutonium-thorium fuel.

The current target exit burnup is approximately 40 MWd/kg. In order to achieve this burnup linear element ratings (LER) will have to remain relatively low (compared to CANDU LER) to reduce the fission gas release. Alternatively, a large amount of free space could be provided to accommodate the fission gas released. Pressurized Water Reactor (PWR) experience suggests that one of the factors for success with high burnup fuel has been to keep LER <40 kW/m (for a solid-rod-type fuel). This well proven approach is adopted as an objective in the fuel design presented here.

LER are limited in solid-rod-type fuel simply to keep fuel temperature lower so the fuel pellet retains more fission gas. It is a means to an end. The actual goal is to keep the fuel cool. The traditional approach to reduction of LER is to increase the sub-division of elements by reducing their diameter. The same amount of power is generated by a larger number of elements and hence the individual element rating is decreased. Internally-cooled annular fuel is a novel approach which achieves fuel temperature reduction by greatly reducing the distance between the centreline of the fuel and a cooled surface and providing a greater surface area for heat transfer.

2. Calculation of Linear Element Ratings

In order to calculate the linear element ratings for the SCWR fuel bundles, the power profile along the fuel channels must first be determined. This requires a model of the whole reactor core, along with an associated refuelling scheme. The radial and axial power profiles for the core can then be used to identify the highest power channel from which the maximum linear element ratings can be calculated.

The full core model was created using the two-group, three-dimensional neutron diffusion code RFSP version 3.5.1 [3]. Cell averaged cross-sections for the 54-element bundle design were used as input to the RFSP model, and were determined from calculation results of the lattice code WIMS-AECL version 3.1 [4], [5] with the ENDF/B-VI nuclear data library. The most current core model consists of 336, 5 metre long fuel channels. Axial properties of the full length fuel assemblies are determined by treating the fuel as ten 0.5 m length sections. This accounts for changes in neutronic behaviour due to variation in coolant properties along the fuel channel.

The proposed refuelling scheme for the SCWR is a three-batch scheme. One third of the core is replaced with fresh fuel at the end of each operating cycle, another third of the core contains once-irradiated assemblies, and the remaining third contains assemblies that have been in core for two cycles. The locations of these fresh, one and two cycle assemblies are determined by a fuel loading scheme. A typical goal of designing such a scheme is to ensure an even power distribution radially across the core, that is, reducing the radial power peaking factor (PPF), defined as the ratio of maximum channel power to average channel power for the reactor. For the proposed reactor power of 2540 MW_{th}, the average channel power will be 7560 kW.

At this stage, no reactivity devices have been modelled nor has any burnable neutron absorber (BNA) been added to fresh fuel or moderator for reactivity suppression. Figure 1 shows the refuelling scheme used for the analysis. This scheme produces a relatively even radial power distribution with power peaking factor of 1.28 and was used in the subsequent LER analysis. It is expected that further refinement to the fuelling scheme, in combination with BNA addition to fresh fuel and reactivity devices will reduce the radial power peaking further.

Table 1: Summary of full-core model results

Parameter	Value
Cycle Length	610 FPD
Excess reactivity at Beginning of Cycle (BOC)	96 mk
Excess reactivity at End of Cycle (EOC)	9 mk
Maximum Bundle Power (BOC)	1311 kW
Maximum Bundle Power (EOC)	1034 kW
Maximum Channel Power (BOC)	9648 kW
Maximum Channel Power (EOC)	8879 kW

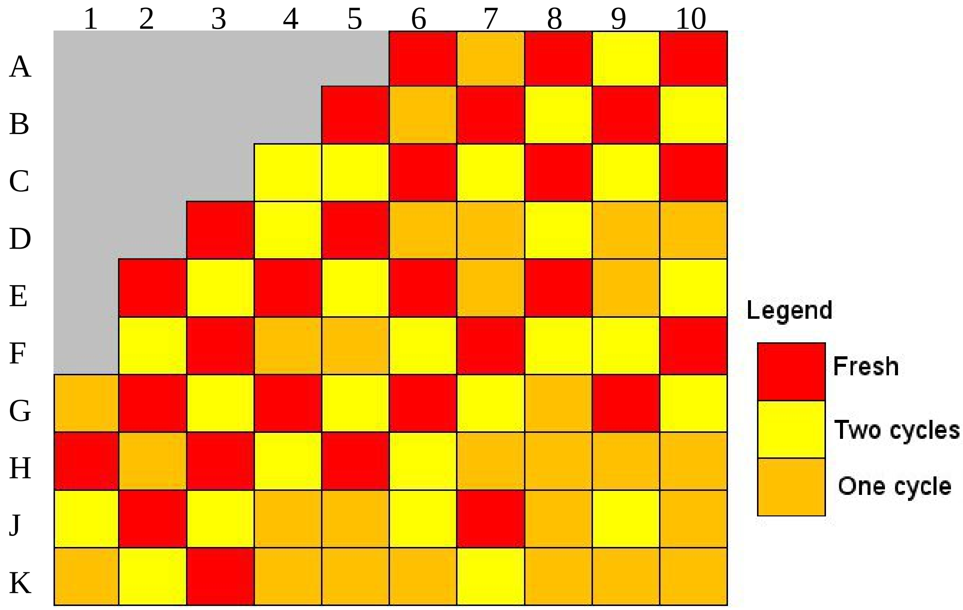

Figure 1: Quarter core fuel loading pattern

The axial power profile used for the LER analysis of the high power channel is shown in Figure 2. This channel is a fresh fuel channel, S11, C10 in the quarter-core map above, was chosen so that the highest LERs in the reactor would be computed. The power of this channel is 9648 kW at BOC.

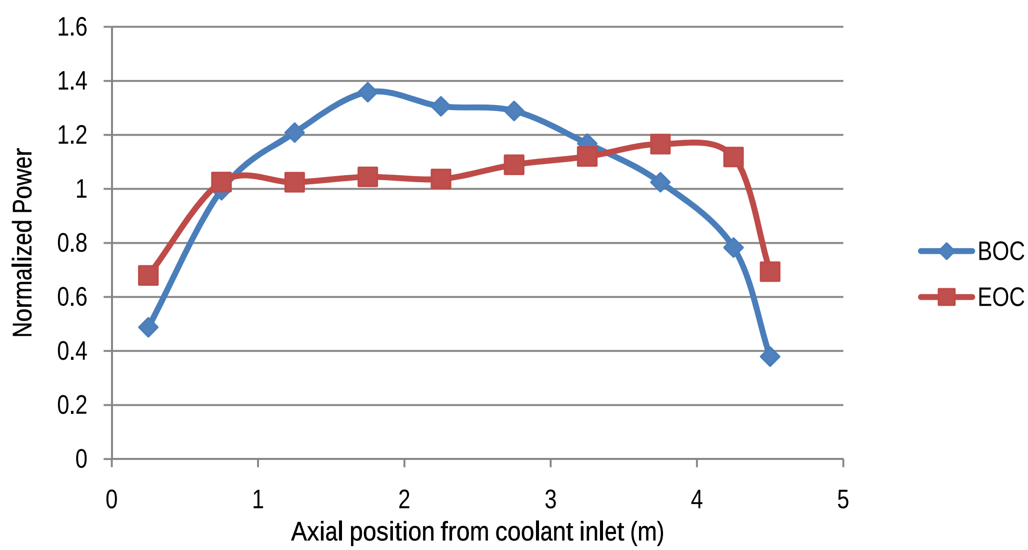

Figure 2: Axial power profile of maximum power channel

The refueling scheme and axial power profiles from RFSP were used to create a power profile to feed back into WIMS-AECL to calculate linear element ratings. The power history was broken up into twelve steps for each of five modeled axial positions, as shown in Figure 3. The same power profile was used for each bundle design.

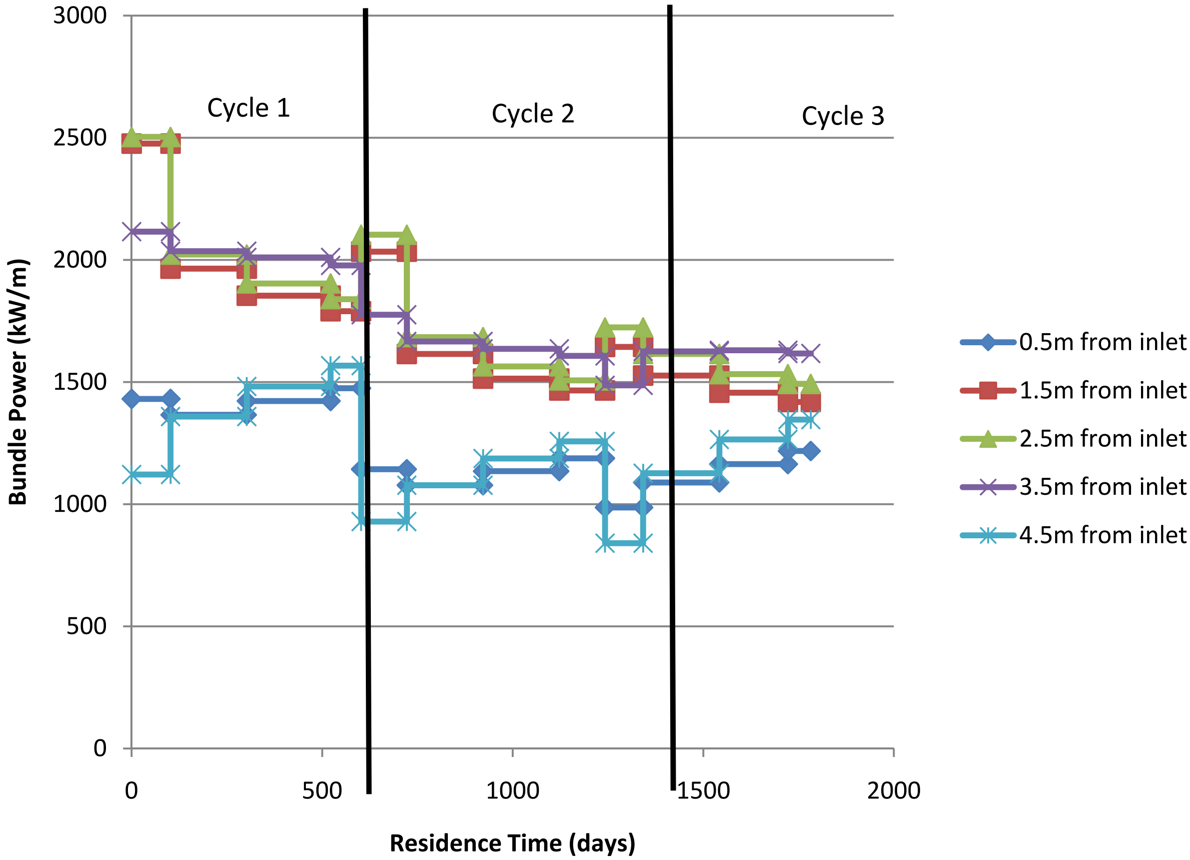

Figure 3 Power profile applied to each axial position.

3. 54-Element Bundle Design

3.1 Overview of the 54-Element Bundle Design

Much of the previous work has used a 54-element bundle design [1], [2]. This bundle has been used with two channel concepts, a high-efficiency channel (HEC) and a re-entrant channel (REC) as described in [6]. For this study the HEC was used with plutonium-driven thorium fuel. The 54-element design has three concentric rings of fuel, with 12, 18, and 24 fuel elements, as shown in Figure 4. This bundle has a large non-fuel region in the centre. For this analysis, this region is composed of zirconia surrounded by cladding. The removal of fuel from the central region of the bundle has the effect of significantly reducing the coolant void reactivity without requiring burnable neutron absorbers [7], [8]. The features of this bundle have been described elsewhere [1].

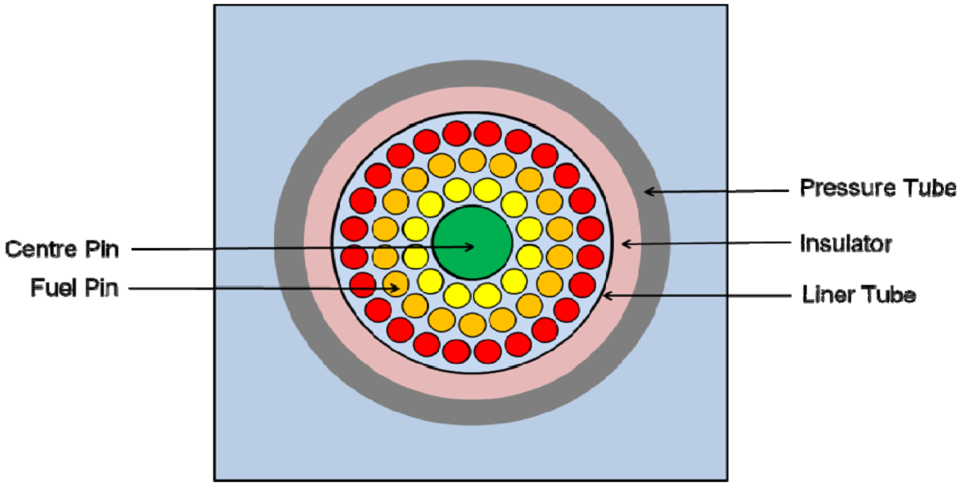

Figure 4 SCWR 54-Element Bundle Design and High Efficiency channel (HEC) lattice cell.

The apparent physics characteristics of this bundle differ slightly from previous studies (e.g. [2]). While previous studies used a flat power distribution in time and axial position, the present studies use a more realistic power distribution that varies both with time and axial position. Interestingly, use of the more realistic power distribution in the models results in an increase in the exit burnup of the fuel. The percentage of plutonium in the fuel was therefore decreased to maintain an exit burnup of around 40 MWd/kg. This bundle uses 12% Pu mixed with the thorium. The plutonium is reactor-grade, from reprocessed light water reactor used fuel.

3.2 Linear Element Ratings of the 54-Element Bundle Design

The values for linear element ratings at each axial location are given in Figure 5. The axial profiles for exit burnup and CVR are shown in Figure 6. The average exit burnup for the channel is 42.1 MWd/kg, and the average CVR is -2.4 mk. The maximum linear element rating of 76.8 kW/m (discussed in Section 3.3) occurs in the outer fuel ring for the fresh fuel at both the 1.5 m and 2.5 m axial positions.

3.3 Linear Element Rating Limits

As mentioned, LER are limited (in general) to keep fuel temperature lower to reduce the amount of fission gas released. A gas release vs. element rating curve for UO_2 is shown in Figure 7 and a gas release vs. burnup curve for UO_2 is shown in Figure 8 [9]. These graphs are based on data from fuel operating under pressurized heavy water reactor (PHWR) conditions (10 MPa heavy-water coolant and 300°C). Gas release is a mainly function of fuel temperature (element rating) and burnup but temperature is the dominant effect. There are other factors that effect gas release such as the detailed power history, microstructure, density, etc. but in general the release rate increases rapidly above 45 kW/m in rod-type UO_2 fuel.

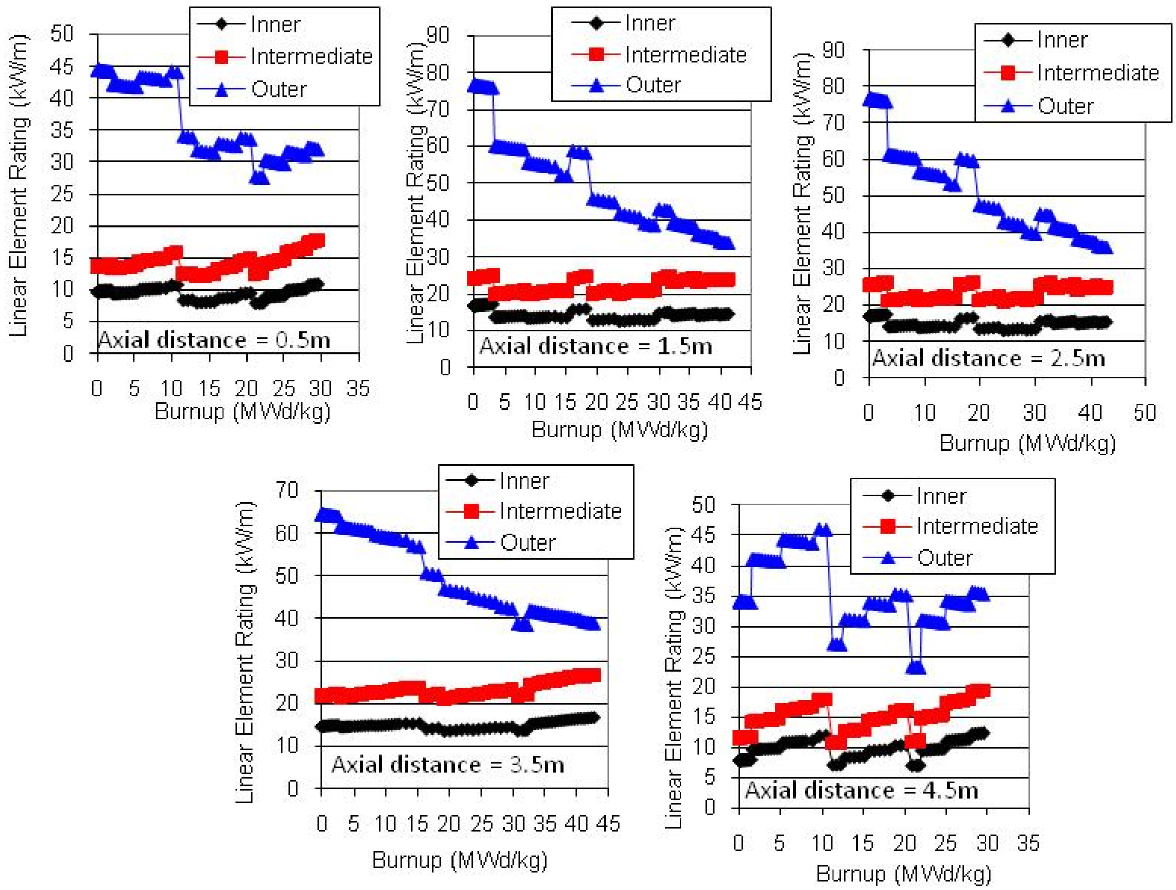

Figure 5 Linear element ratings for the 54-element design

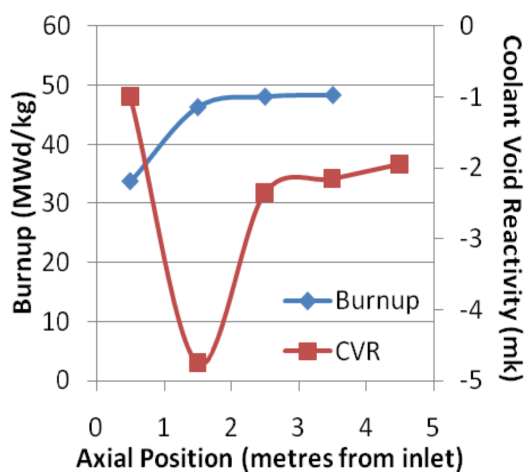

Figure 6 Exit burnup and coolant void reactivity as a function of axial position along the channel.

The reference fuel in the Canadian SCWR is thoria/plutonia. Pure thoria has a significant improvement in thermal conductivity compared to UO_2 but this improvement degrades with the addition plutonia. No data is available on the thermal properties of thoria containing large amounts of plutonia so the improvement in thermal conductivity, if any, is unknown. In addition, thoria is more refractory than UO_2 and therefore fission gas diffusion/release is probably better than UO_2 for equivalent operating temperatures. Unfortunately this property will also be degraded with the addition of large amounts of plutonia. Since SCWR fuel is operating with higher coolant temperatures compared to PHWRs the fuel itself will also operate with this increased step in temperature. The coolant temperature changes considerably along the SCWR channel (350 to 625°C) but if we consider an average increase of 200°C compared to PHWR conditions then the gas release curves given in Figure 7 should be adjusted by -5 kW/m. Using the adjusted UO_2 database as a reference for gas release in this thoria/plutonia fuel is considered to be a conservative approach. Based on the rational presented here a LER maximum of 40 kW/m for solid-rod type fuel in a PT-SCWR is suggested as a design objective.

In UO_2 fuel, columnar grain growth starts at approx. 65 kW/m and central melting at 80 kW/m. Central melting of the fuel under normal operating conditions would not be permitted as a design requirement. As mentioned, the thermal properties and melting point of this thoria/plutonia fuel are not known but if we use UO_2 as a reference, clearly the maximum powers predicted in the 54-element design are not acceptable.

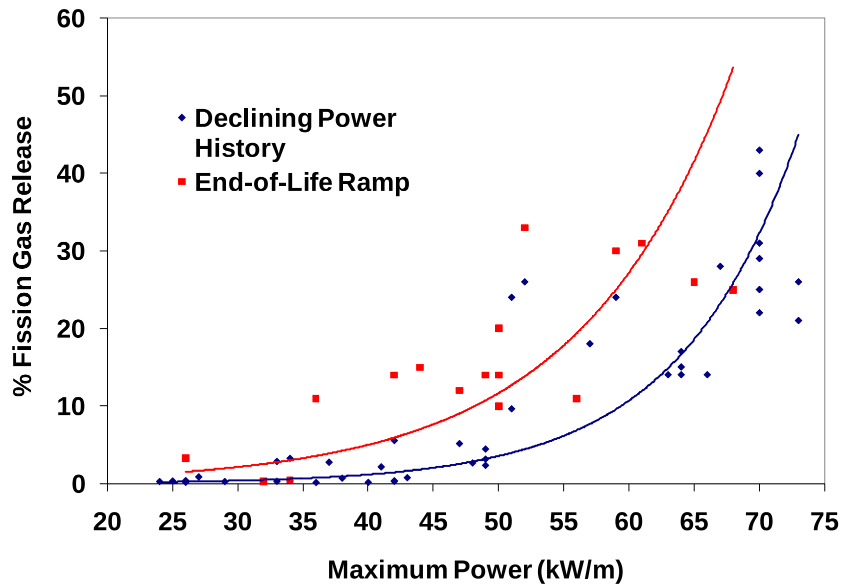

Figure 7 Fission Gas Release (FGR) vs. maximum element linear power [9]

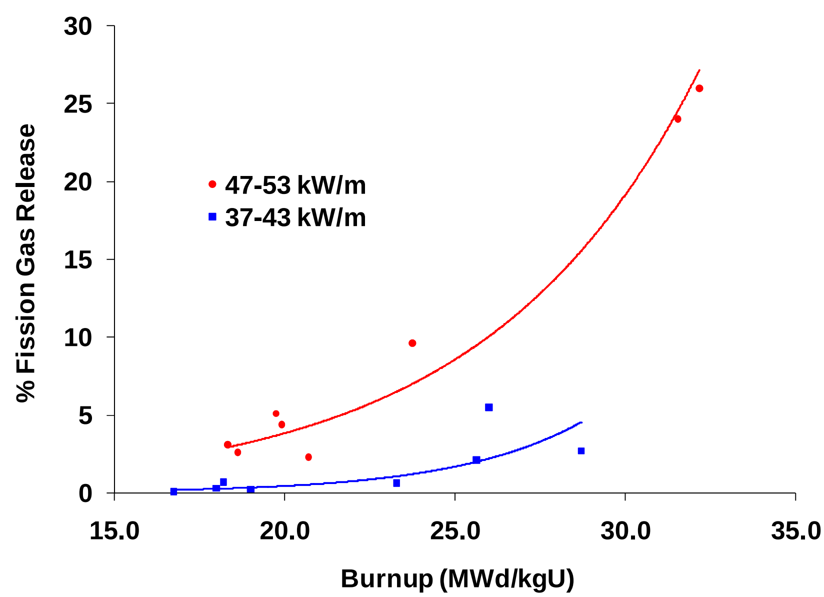

Figure 8 Fission Gas Release (FGR) vs. burnup [9]

4. Subdivided Bundle Design

4.1 Overview of Subdivided Bundle Design

In this bundle design the pins in the outer rings are subdivided as shown in Figure 9, in order to lower the LER in the outer ring. The pellet radius is 3.5mm [10], and bundle geometry is given in Table 2. The liner tube, insulator, and pressure tube are kept the same as in the 54-element design, and the inner two rings of fuel pins are moved out. The centre pin is also correspondingly larger. As a result of the larger pitch circle radii, there are more fuel elements in rings 1 and 2 than in the 54-element design. Subdividing the fuel, using more pins of smaller diameter, also decreases the overall fuel mass of the bundle and increases the non-fuel mass. The mass of fuel in the channel with this bundle is 254 kg, versus 278 kg for the original 54-element design. Since there is now relatively more (neutron absorbing) non-fuel mass in the bundle, an increase in plutonium composition was required to maintain the same exit burnup as the 54-element design. The fuel composition for the subdivided bundle is increased from 12% to 13% plutonium in thorium.

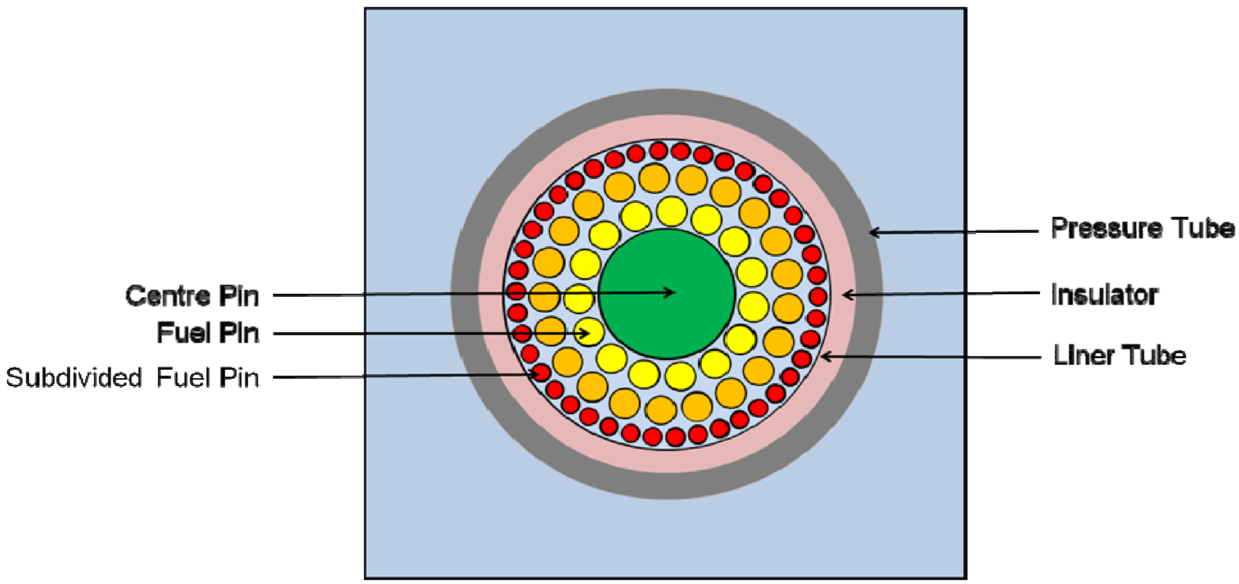

Figure 9 Fuel bundle design with subdivided fuel pins in the outer ring.

Table 2 Geometry parameters for the subdivided fuel bundle design.

Parameter	Value
Lattice Pitch	25 cm
Elements per bundle	78
Elements in rings 1, 2, 3	15, 21, 42
Pitch circle radius, ring 1	3.655 cm
Pitch circle radius, ring 2	5.11 cm
Pitch circle radius, ring 3	6.295 cm
Radius of central pin	2.82 cm
Outer radius of central pin cladding	2.88 cm
Radius of pins in ring 1 and 2	0.62 cm
Outer radius of ring 1 and 2 pin cladding	0.68 cm
Radius of pins in ring 3	0.35 cm
Outer radius of ring 3 pin cladding	0.41 cm
Liner Tube inner radius	6.8 cm
Liner Tube thickness	0.05 cm
Insulator inner radius	6.85 cm
Insulator thickness	1.0 cm
Pressure tube inner radius	7.85 cm
Pressure tube thickness	1.2 cm

4.2 Linear Element Ratings of Subdivided Bundle Design

The values for linear element ratings at each axial location over the predicted burnup range are given in Figure 10. The axial profiles for exit burnup and CVR are shown in Figure 11. The average exit burnup for the channel is 43.1 MWd/kg, and the average CVR is 0.1 mk. The maximum linear element rating of 37 kW/m occurs in the intermediate fuel ring for the fresh fuel at the 2.5 m axial position. As the maximum LER has moved to the intermediate ring in this fuel design, this indicates that the bundle may be able to use slightly larger diameter fuel elements in the outer ring. The maximum linear element ratings for the intermediate and outer rings are similar for this design. These LER appear to be compatible with the target burnup.

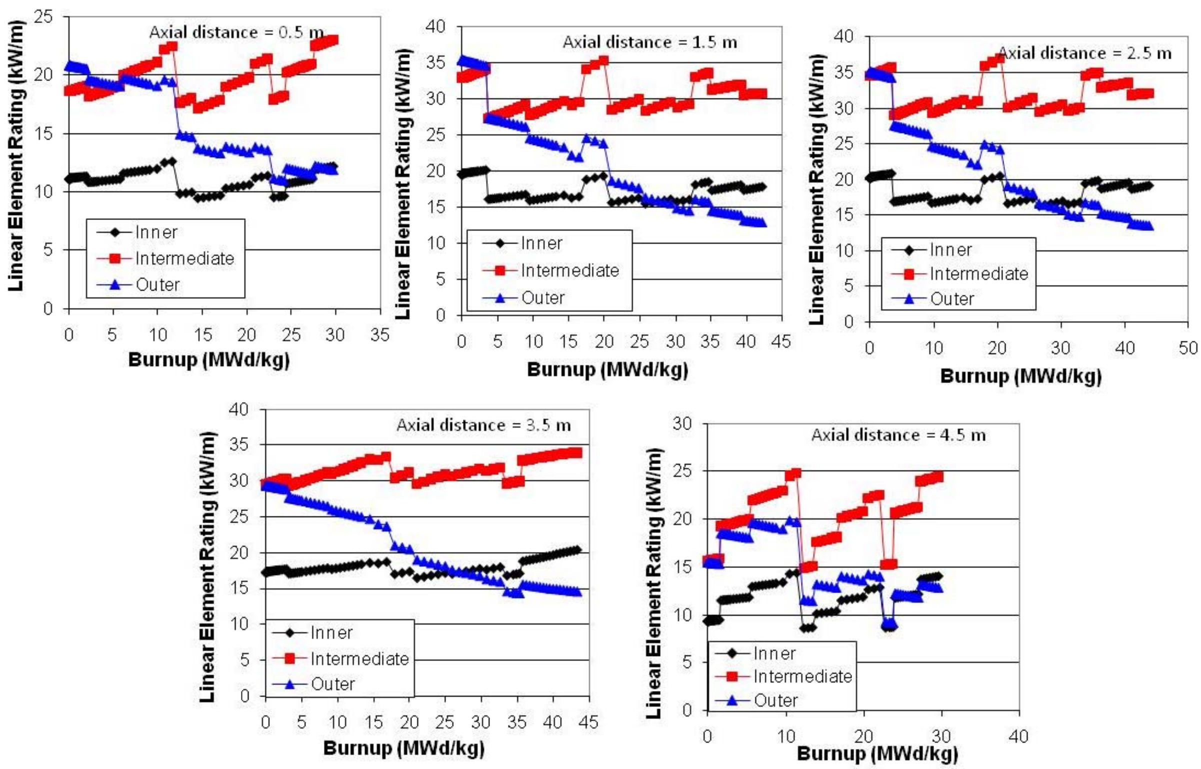

Figure 10 Linear element ratings at 0.5 m from the inlet for the subdivided fuel bundle design

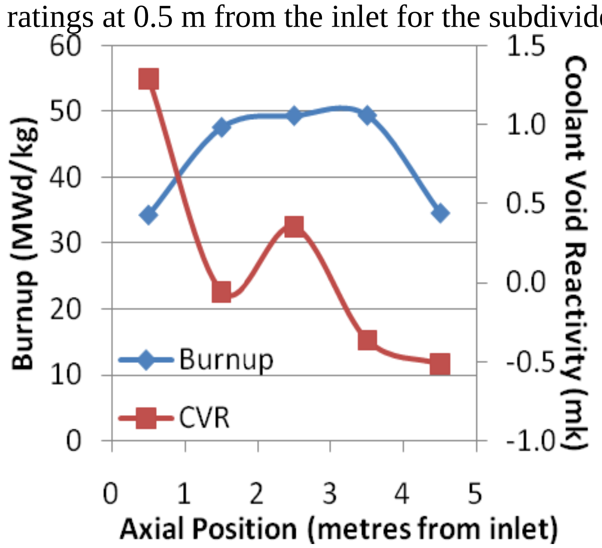

Figure 11 Exit burnup and coolant void reactivity as a function of axial position along the channel.

5. Internally-Cooled-Annular Fuel Bundle Design

5.1 Internally-Cooled-Annular Fuel Elements

The internally cooled annular fuel (ICAF) design can be thought of as a variation on element subdivision. Instead of smaller individual elements, the ICAF element can be though of as a group of smaller elements that are arranged in a ring with a common clad. The power is distributed, as in sub-division, but instead of an unrealistically small pin size one gets the structurally robust double walled element.

The main advantage of ICAF is the relative reduction in fuel temperature for equivalent power output. Consider the solid-rod fuel design where the maximum distance between fuel and a cooled surface is equal to the pellet radius; 6.2 mm in the 54 element design and 3.5 mm in the small pin of the subdivided case above. In the ICAF case presented here the maximum distance between fuel and a cooled surface is 2.45 mm, a 60% and 30% reduction compared to the 54 and small pin cases above. Consider also the total cooled surface area available for heat transfer in the outer rings of the three designs. The relative cooled surface area ratios for the 54, small pin and annular designs are 0.6 : 0.6 :1.0 respectively. The positive aspect of more surface area to transfer heat to the coolant must be weighed against an undesirable increase in neutron absorbing cladding material. The results presented in Section 5.2 suggest that the increase in cladding material did not have a significant effect in the overall bundle design (burnup and plutonium concentration).

Finite element analysis was performed to estimate fuel temperature distribution in the ICAF. It should be noted that this model does not include a gap between the fuel and the cladding and therefore the results are expected to be optimistic in this regard. Conversely, the uniform thermal conductivity value used (3 W/m·K) is conservative for UO_2 over this temperature range and will result in predicted temperatures higher than those expected in real fuel. The analysis was done at the outlet temperature condition (i.e. the maximum temperature and therefore conservative). Future work involves refining the model to include a fuel-clad gap. The analysis was performed for two linear element ratings; 80 and 120 kW/m. Results are shown in Figure 12 and Figure 13. The maximum fuel temperatures are 870°C and 1100°C respectively. In solid-rod-type fuel operating under PHWR conditions equivalent centreline temperatures would occur at LERs of approximately 28 and 35 kW/m respectively.

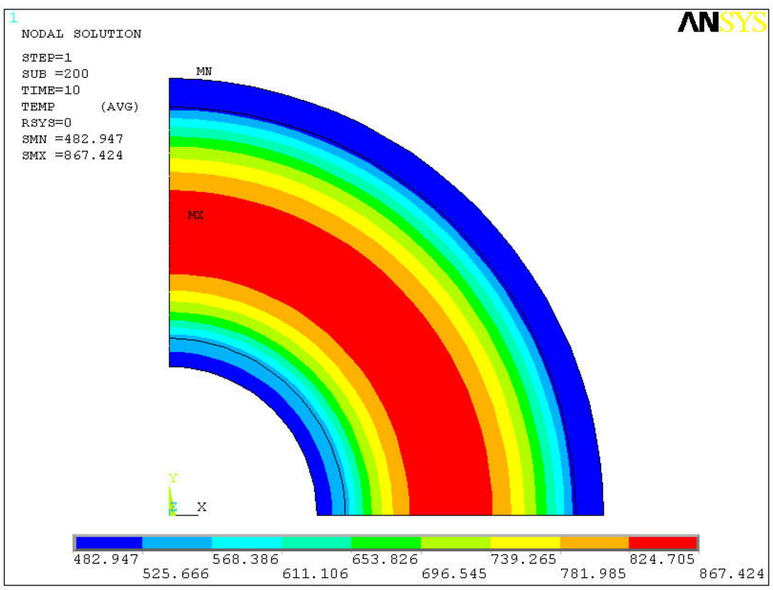

Figure 12 Thermal analysis of SCWR ICAF at 80 kW/m (no fuel-clad gap)

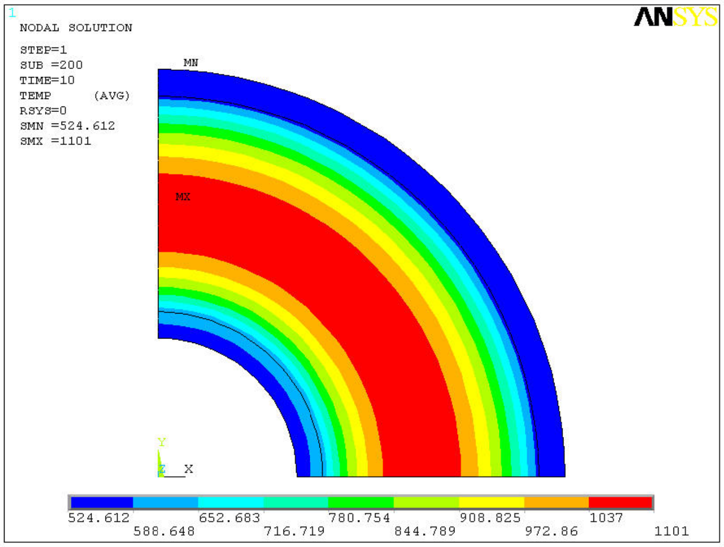

Figure 13 Thermal analysis of SCWR ICAF at 120 kW/m (no fuel-clad gap)

5.2 Overview of Internally-Cooled-Annular Fuel Bundle Design

Since the maximum linear element ratings occur in the outer ring for the 54-element design, with the ratings for the inner two rings being significantly lower, annular fuel was only used in the outer ring of this bundle design. As a first attempt to design a bundle containing annular fuel elements, the geometry of the bundle was selected to have approximately the same fuel mass in the outer ring as the 54-element bundle design, and the hole size in the centre of the pellet was chosen to be approximately equal to the thermalhydraulic diameter of the bundle (see Figure 14). The outer diameter of the fuel pellet is thus larger than for the 54-element design. As a result, the liner tube, insulator, and pressure tube diameters were expanded, Table 3. As a consequence of relocation of the fuel to larger radial distances in the bundle, the coolant void reactivity of the bundle decreased. The lattice pitch was expanded to 26 cm to bring the coolant void reactivity up to a similar level as the 54-element design. The increase in lattice pitch resulted in an increase in exit burnup, so the plutonium concentration in the fuel was decreased in order to have a comparable exit burnup to the 54-element design. As with the 54-element design, the fuel composition for this bundle is 12% Pu mixed with thorium.

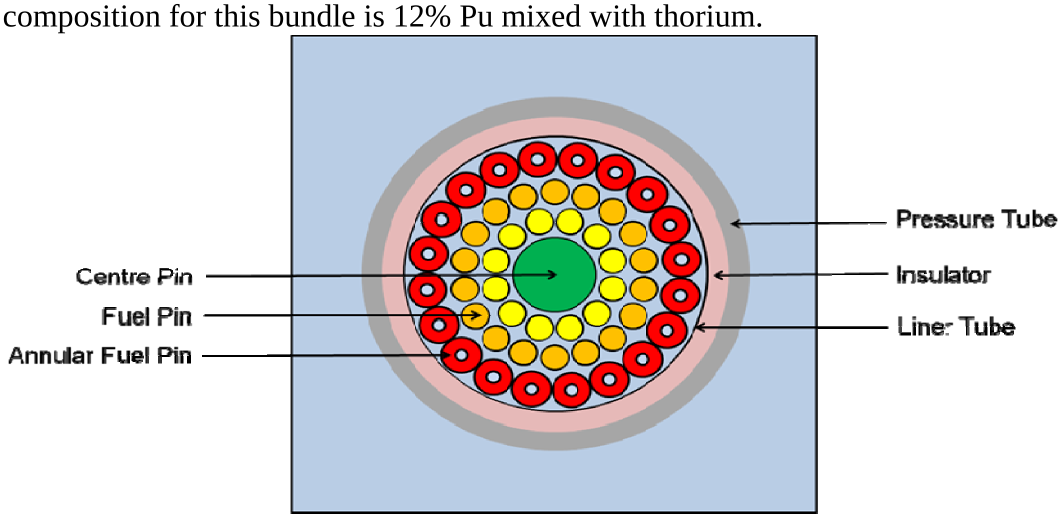

Figure 14 Fuel bundle design with internally-cooled annular fuel in the outer ring.

Table 3 Geometry parameters for the fuel design with annular fuel.

Parameter	Value
Lattice Pitch	26 cm
Elements per bundle	50
Elements in rings 1, 2, 3	12, 18, 20
Pitch circle radius, ring 1	2.8755 cm
Pitch circle radius, ring 2	4.3305 cm
Pitch circle radius, ring 3	6.1 cm
Radius of central pin	1.94 cm
Outer radius of central pin cladding	2.00 cm
Radius of pins in ring 1 and 2	0.62 cm
Outer radius of ring 1 and 2 pin cladding	0.68 cm
Inner Radius of pins in ring 3	0.375 cm
Inner radius of ring 3 pin cladding	0.315 cm
Outer Radius of pins in ring 3	0.865 cm
Outer radius of ring 3 pin cladding	0.925 cm
Liner Tube inner radius	7.2 cm
Liner Tube thickness	0.05 cm
Insulator inner radius	7.25 cm
Insulator thickness	1.0 cm
Pressure tube inner radius	8.25 cm
Pressure tube thickness	1.2 cm

5.3 Linear Element Ratings of Annular Fuel Bundle Design

The values for linear element ratings, burnup and coolant void reactivity at each axial location are given in Figure 15. The axial profiles for exit burnup and CVR are shown in Figure 16. The average exit burnup for the channel is 41.6 MWd/kg, and the average CVR is -0.8 mk. The maximum linear element rating of 99 kW/m occurs in the outer fuel ring for the fresh fuel at the 2.5 m axial position. Based on the maximum fuel temperatures from the analysis of ICAF given in Section 5.1, the maximum fuel temperature for an ICAF element operating at 100 kW/m would be approximately 1000°C. This is equivalent to a solid-rod-type fuel element operating a 33 kW/m under PHWR conditions and is therefore considered acceptable for high burnup applications.

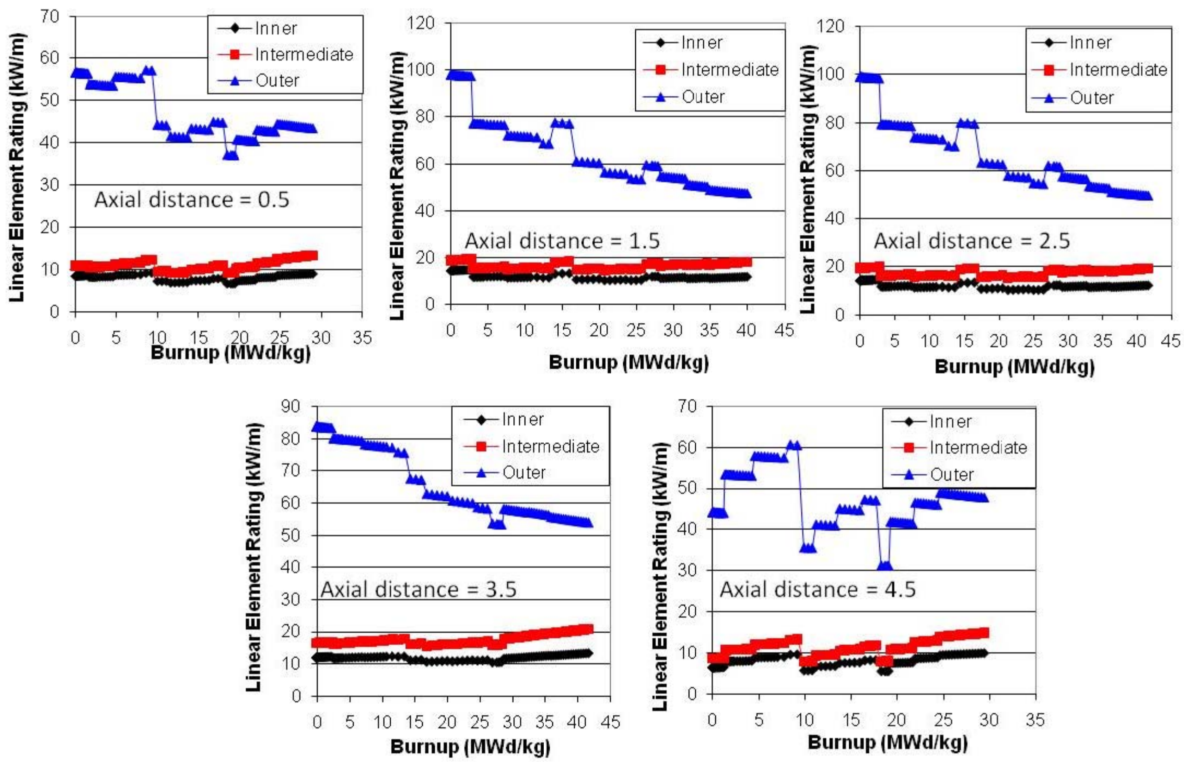

Figure 15 Linear element ratings at 0.5 m from the inlet for the annular fuel bundle design

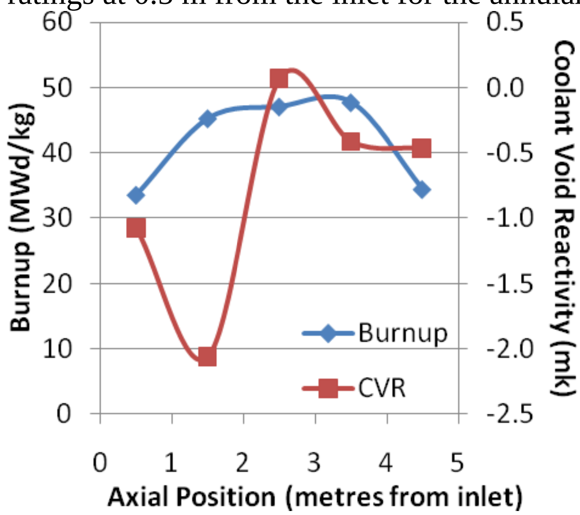

Figure 16 Exit burnup and coolant void reactivity as a function of axial position along the channel.

6. Comparison of the Three Fuel Designs

The major characteristics of the three fuel designs are show in Table 4. The exit burnup and CVR for the three designs are similar. The coolant void reactivity of all three designs is slightly higher than desired, and higher than reported in previous studies, where the CVR is usually around -5 mk. An increase in CVR was observed in this study, where the power profile was varied along the channel. As the channel design for the SCWR is developed further the lattice pitch can be decreased slightly or a small amount of burnable neutron absorber can be added to the centre pin in order to lower the CVR to the desired value.

Table 4 A comparison of the three fuel bundle designs for exit burnup, CVR, maximum linear element rating and maximum fuel temperature.

Parameter	54-Element	Subdivided Outer Ring	Annular Outer Ring
Exit Burnup (MWd/kg)	42.1	43.1	41.6
Coolant Void Reactivity (mk)	-2.4	0.1	-0.8
Maximum Linear Element Rating (kW/m)	77	37	99
Approximate Maximum Fuel Temperature (°C)	2850 (possible melting)	1400	1000

7. Thermalhydraulics Characteristics of the Three Fuel Designs

A detailed assessment of the thermalhydraulics characteristics of the three bundle designs is being carried out. In the mean time, a hot-pin calculation has been performed assuming cross-sectional average flow conditions at the peak power pin. The heat-transfer coefficient is calculated with

$$HTC = \frac{kNu}{D_{he}} \tag{1}$$

where k is the thermal conductivity in W·m^{-}1·K^{-1}. D_{he} is the heated-equivalent diameter in meters and expressed as

$$D_{he} = \frac{4\,A_{flow}}{P_{he}} \tag{2}$$

where P_{he} is the heated perimeter and expressed as

$$P_{he} = \pi(D_c + n_{R1}D_{R1} + n_{R2}D_{R2} + n_{R3}D_{R3}) \tag{3}$$

The flow area (A_{flow}) in m^2 is calculated as

$$A_{flow} = \frac{\pi}{4}D_{liner}^2 - D_{ele}^2 \tag{4}$$

with

$$D_{ele}^2 = \frac{\pi}{4}(D_c^2 + n_{R1}D_{R1}^2 + n_{R2}D_{R2}^2 + n_{R3}D_{R3}^2) \tag{5}$$

where n_{R1}, n_{R2} and n_{R3} are the numbers of elements in Ring 1, Ring 2 and Ring 3, respectively, and D_c, D_{R1}, D_{R2} and D_{R3} are the diameters of pins including cladding in meters in the center, and in Ring 1, Ring 2 and Ring 3, respectively.

The Nusselt number Nu in Equation 1 was calculated using the conventional Dittus-Boelter correlation:

$$Nu = 0.023\,Re^{0.8}Pr^{0.4} \tag{6}$$

where Re is the Reynolds number, defined as

$$Re = \frac{G\,D_{hyd}}{\mu} \tag{7}$$

with μ being the dynamic viscosity in Pa·s^{-1}. D_{hyd} is the hydraulic diameter in meters and expressed as

$$D_{hyd} = \frac{4\,A_{flow}}{P_{wet}} \tag{8}$$

where P_{wet} is the wetted perimeter and expressed as

$$P_{wet} = \pi(D_{liner} + D_c + n_{R1}D_{R1} + n_{R2}D_{R2} + n_{R3}D_{R3}) \tag{9}$$

The mass flux (G) in Equation 7 is calculated by

$$G = \frac{\dot{m}}{A_{flow}} \tag{10}$$

with $\dot{m}$ being the mass flow rate in kg·s^{-1}. The Prandtl number (Pr) in Equation 6 is expressed as

$$Pr = \frac{C_p\mu}{k} \tag{11}$$

where C_p is the specific heat in J·kg^{-1}·K^{-1}. Data from NIST Standard Reference Database *NIST Chemistry WebBook* [11] was used for the calculation of supercritical water properties.

The channel flow rate is calculated using the average channel power (7560 kW, section 2) and the enthalpy increase along the channel. Since the detailed of the fuel design (e.g., spacer configuration) had not finalized yet, the hydraulic characteristic of the channel has not been identified. Therefore, it is assumed that the pressure drop along the channel is 1 MPa and the pressure at the inlet is 26 MPa.

$$\dot{m} = \frac{Average\ Channel\ Power}{(H_{out} - H_{in})} \tag{12}$$

where H_{in} and H_{out} are the enthalpies at the entrance and exit in kJ·kg^{-1}, respectively, corresponding to the fluid temperatures of 350°C and 625°C. The enthalpies are calculated as a function of pressure and temperature. The calculated mass flow rate in the channel, having an average power of 7560 kW, is 3.89 kg·s^{-1}.

Figure 17 illustrates the axial heat-flux profiles of the outer-ring pin for the three bundle designs with fresh fuel (the most limiting). All profiles exhibit an upstream-skewed shape with the peak located at around 1.8 metres from the inlet end, which is downstream of the pseudo-critical location at around 1.2 metres.

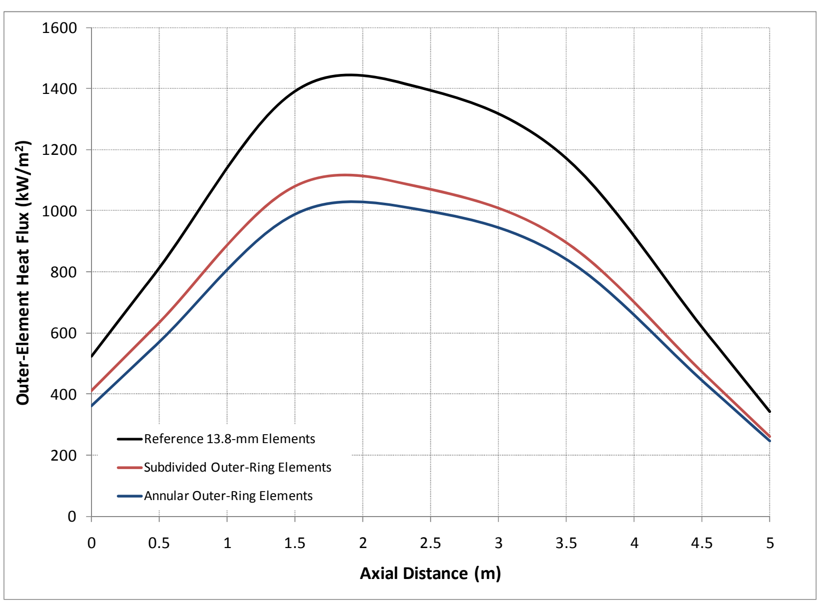

Figure 17 Axial Heat-Flux Profiles of the Outer-Ring Pin

Table 5 summarizes the flow parameters of the three bundle designs. Flow areas of the 54-element bundle and outer-channel of the annular fuel bundles are quite similar, but the flow area of the subdivided outer-ring-element bundle is smaller than the other two designs. The mass flux, on the other hand, is higher for the subdivided outer-ring-element bundle and is the lowest for the inner channel of the outer-ring element in the annular fuel bundle. As indicated in the footnote, the mass flux distribution between inner and outer channels of the annual fuel bundle has been established using the constant pressure-drop calculation based on an assumed friction factor for both channels. In view of the presence of spacers in the outer channel of the annular fuel bundle, the mass flux in the inner channel may be underestimated. Corresponding to the mass flux variations, the HTCs calculated with the inlet or outlet flows are also higher for the subdivided outer-ring-element bundle than those for the other two designs. Combining with the lower peak pin heat flux, the heat transfer characteristic is anticipated to be better for the subdivided outer-ring-element bundle than those for the other two designs. Similarly, the heat transfer characteristic is anticipated to be the worst for the reference 54-element bundle due to the high peak pin heat flux and relatively low mass flux.

Figure 18 illustrates the predicted axial cladding temperature distributions at the outer-ring element of the three bundle designs. Peak cladding temperatures have been observed at locations between 3.5 and 4.5 metres even though the peak heat fluxes are located at around 1.8 metres. The highest peak cladding temperature is 794°C for the reference bundle design having 54 13.8-mm elements. The lowest peak cladding temperature is 707°C for the subdivided outer-ring-element bundle design. Cladding temperatures for the annular fuel bundle design lie between those of the reference and subdivided outer-ring-element bundle designs. Those at the inner channels of the outer-ring elements in the annular fuel bundle design are close to cladding temperatures of the subdivided outer-ring-element bundle design. As indicated previously, the predictions are based on the hot pin heat flux and the cross-sectional average flow conditions. These values are considered preliminary and are presented for comparison purpose only. Detailed subchannel analyses are in progress to optimize various bundle designs.

Table 5 Comparison of Thermalhydraulics Characteristics of the Bundle Designs

Outer-Ring Pin Design	**Flow Area (m^2)**	**Mass Flux ($kg \cdot m^{-2}s^{-1}$)**	**Peak Pin Heat Flux ($kW \cdot m^{-2}$)**	**HTC[1] ($W \cdot m^{-2}K^{-1}$)**	**HTC[2] ($W \cdot m^{-2}K^{-1}$)**
54 element (Ref. 13.86-mm)	0.005426	717.0	1394.5	13086.3	4470.5
Subdivided	0.004473	869.6	1079.8	16261.5	5555.2
Annular-Outer channel	0.005295[3]	660.8[4]	997.8	12456.6	4255.4
Annular-Inner channel	0.000623[5]	626.6	997.8	13857.6	4734.0

[1] HTC was calculated using the water properties at 26 MPa and 350°C.
[2] HTC was calculated using the water properties at 25 MPa and 625°C.
[3] Flow area was calculated excluding the inner flow channel of the outer-ring pin.
[4] Approximate value based on pressure-drop calculations of an assumed friction factor for inner and outer channels.
[5] Flow area was calculated for the inner flow channel of all outer-ring pins.

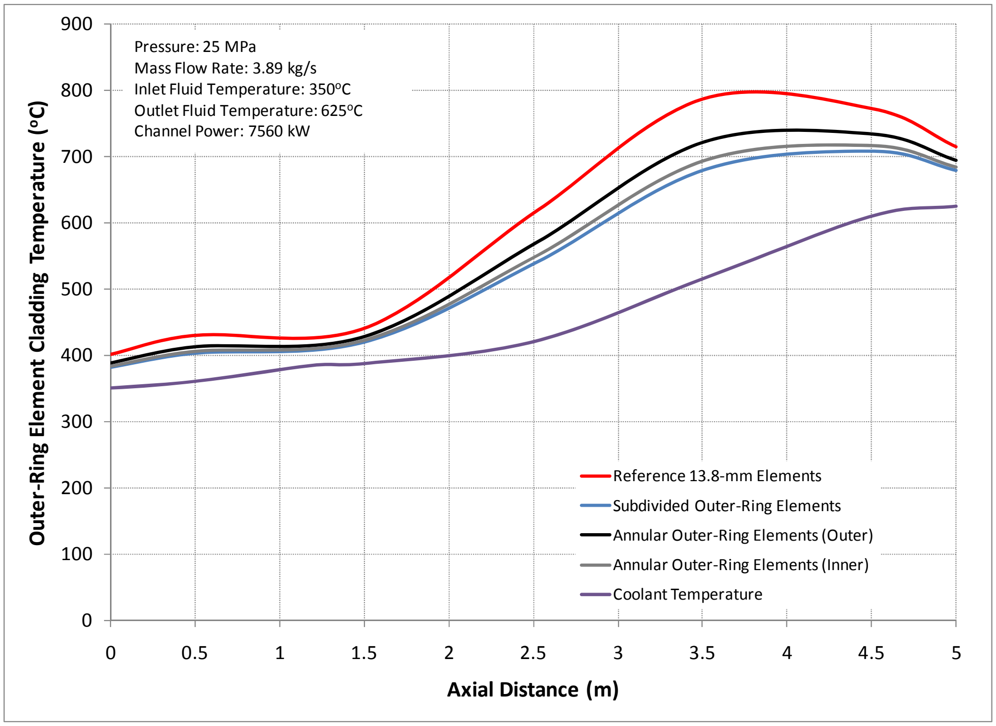

Figure 18 Outer-Ring Element Cladding Temperatures Based on Preliminary Hot-Pin Calculations for Three Bundle Designs.

8. Conclusions

The current target burnup of the Canadian SCWR is 40 MWd/kgHE. This burnup is well within the experience base for UO_2 solid-rod-type fuel. In general, high-burnup fuels have operated at relatively low LER in order to keep fuel temperature such that large amounts of fission gas are not released. Since the thermal properties of the reference thoria/plutonia fuel are not known the fuel is assumed to behave like UO_2 and have similar gas release and fuel temperature behaviour. Given the higher melting point and better thermal conductivity of pure thoria compared to UO_2 this is considered to be a conservative approach. Based on the gas release data for UO_2 operating under PHWR conditions but adjusted for the higher operating temperature of the SCWR, a maximum linear element rating of 40 kW/m for any solid-rod-type fuel is adopted as a design objective. There are several aspects of the fuel design which are unknown at this time. One of these aspects, which may affect element rating limits, is sheath collapse. For reasons such as these a more appropriate design objective might be a maximum fuel temperature. If we again use the UO_2 data as a reference then the centreline temperature in fuel with mid-burnup (20 MWd/kgU) at 45 kW/m operating under PHWR conditions would be approximately 1500°C. This 1500°C maximum fuel temperature could be considered as an alternative design objective.

The ICAF design offers the advantages of decreased maximum fuel temperature and a potentially more robust structural design but has the drawbacks of increased cladding material and a general lack of experience with the design.

From a fuel performance perspective both the subdivided and ICAF designs appear to be acceptable. The high LER and hence fuel temperature of the 54 element design make it unviable.

From thermalhydraulics point of view, the preliminary analysis using the hot-pin calculation showed that the peak cladding temperature is lower for the subdivided outer-ring-element bundle design than those of other designs. The highest peak cladding temperature has been observed for the reference 54-element bundle design. Detailed analyses are in progress to optimise the geometry of various designs.

9. References

[1] Boczar, P.G., et al., "Reactor Physics Studies for a Pressure Tube Supercritical Water Reactor (PT-SCWR)", The 2nd Canada-China Joint Workshop on Supercritical Water-Cooled Reactors (CCSC-2010), Toronto, Canada, 2010 April.

[2] Pencer, J, et al., "Thorium Fuel Cycles in the CANDU Supercritical Water Reactor", Proceedings of the 5th International Symposium on Supercritical Water Reactors (these proceedings), Vancouver, Canada,2011 March.

[3] Rouben, B., RFSP-IST, the Industry Standard Tool Computer Program for CANDU Reactor Core Design and Analysis, in Proceedings of 13th Pacific Basin Nuclear Conference (PBNC-2002), Shenzhen, China, (2002).

[4] Altiparmakov, D., New Capabilities of the Lattice Code WIMS-AECL, PHYSOR-2008, International Conference on Reactor Physics, Nuclear Power: A Sustainable Resource, Interlaken, Switzerland (2008).

[5] Irish, J.D., and Douglas, S.R., Validation of WIMS-IST", Proceedings of 23rd Canadian Nuclear Society (CNS-2002) Conference, Toronto, Canada (2002).

[6] Chow, C.K. and Khartabil, H.F., "Conceptual Fuel Channel Designs for CANDU-SCWR", Nuclear Engineering Technology, 40(2): 139-146, 2007.

[7] Roshd, M.H.M, French, P.M., and Jones, R.T., "Nuclear Fuel Bundle Design with Reduced Void Effect", ANS Transactions, 26, 603-604, 1977.

[8] Dastur, A.R. and Buss, D.B., "The Influence of Lattice Structure and Composition on the Coolant Void Reactivity in CANDU", 11th Annual Conference of the Canadian Nuclear Society, Toronto, June 3-6, 1990.

[9] Floyd, M.R., "Extended-Burnup CANDU Fuel Performance", 7th International CANDU Fuel Conference Proceedings, Vol. 2, pp 5A1-5A20, ISBN 0-919784-71-2.

[10] Higuchi, S, Sakurai,S, and Ishida, T, "A Study of Fuel Behaviour in an SCWR Core with High Power Density", Proceedings of ICAPP 2007, Nice, France,2007 May.

[11] National Institute of Science and Technology Chemistry Webbook, http://webbook.nist.gov/chemistry/, 2008.